

Shared strategies for β -lactam catabolism in the soil microbiome

Terence S. Crofts^{1,2}, Bin Wang^{1,2}, Aaron Spivak², Tara A. Gianoulis^{3,10}, Kevin J. Forsberg^{2,8},
 Molly K. Gibson², Lauren A. Johns⁴, Stacey M. Broomall⁴, C. Nicole Rosenzweig⁴,
 Evan W. Skowronski^{4,9}, Henry S. Gibbons⁴, Morten O. A Sommer^{1,2} and Gautam Dantas^{1,2,6,7*}

The soil microbiome can produce, resist, or degrade antibiotics and even catabolize them. While resistance genes are widely distributed in the soil, there is a dearth of knowledge concerning antibiotic catabolism. Here we describe a pathway for penicillin catabolism in four isolates. Genomic and transcriptomic sequencing revealed β -lactamase, amidase, and phenylacetic acid catabolon upregulation. Knocking out part of the phenylacetic acid catabolon or an apparent penicillin utilization operon (*put*) resulted in loss of penicillin catabolism in one isolate. A hydrolase from the *put* operon was found to degrade in vitro benzylpenicilloic acid, the β -lactamase penicillin product. To test the generality of this strategy, an *Escherichia coli* strain was engineered to co-express a β -lactamase and a penicillin amidase or the *put* operon, enabling it to grow using penicillin or benzylpenicilloic acid, respectively. Elucidation of additional pathways may allow bioremediation of antibiotic-contaminated soils and discovery of antibiotic-remodeling enzymes with industrial utility.

The discovery of antibiotics and their development into an armamentarium against bacterial infections has been one of the great public health success stories of the last century. However, increasing antibiotic resistance in pathogenic bacteria with the concomitant decrease in the development of new antibiotics threatens a return to the dark ages of the pre-antibiotic era¹. Bacterial resistance to antibiotics is ancient² and ubiquitous in the environment^{3,4}. Moreover, anthropogenic antibiotic use has led to a measurable increase in carriage of antibiotic resistance genes in the environment with the potential to spread to the clinic⁵.

The ultimate fate of antibiotics in the environment, and what role resistance plays in their mineralization, is unknown. Most antibiotics are natural products, or derivatives thereof, originally isolated from soil bacteria⁶. Given their soil origin, and the lack of environmental accumulation of these organic compounds, it is natural that some antibiotics are consumed by soil bacteria as carbon or nitrogen sources. This was recognized soon after the mass anthropogenic introduction of antibiotics by studies demonstrating the ability of soil bacteria to mineralize various natural antibiotics including streptomycin⁷, penicillin G (also known as benzylpenicillin, referred to hereafter simply as penicillin)⁸, and chloramphenicol⁹. In the literature, utilization of penicillin has most often focused on *Pseudomonas* strains, with conflicting evidence for what part of the molecule is used as a carbon source^{10–12}, although catabolism of penicillins in other organisms, such as *Klebsiella pneumoniae*, has been reported as well¹³. Little is known about the pathways and enzymes used during catabolism, including whether β -lactamase activity is required^{8,11,14}. More recently, the list of antibiotics capable of sustaining bacterial growth has

expanded substantially, as has the catalog of bacterial species capable of subsisting on antibiotics^{14–19}. However, controversy still remains over the characterization of resistant, but not metabolizing, versus subsistent growth phenotypes. To date, no specific genes or pathways have been identified that enable bacteria to use antibiotics as a sole carbon source^{16,20}.

Here we provide evidence for a pathway for β -lactam antibiotic catabolism in which amidases, found to be distinct from known penicillin amidase enzymes, link resistance enzymes to central metabolism. We demonstrate that this strategy can be transferred to *E. coli*, enabling it to grow using penicillin as its sole carbon source. These findings have important implications for antibiotic ecology, bioremediation of antibiotic contaminated sites, and the synthesis of semisynthetic antibiotics.

Results

Proteobacteria using β -lactams as a sole carbon source. Four Proteobacteria soil isolates of the *Burkholderia*, *Pseudomonas*, and *Pandoraea* genera, termed ABC02, ABC07, ABC08, and ABC10 (Supplementary Table 1; ABC, antibiotic catabolizer), were previously isolated from soil by growth in minimal media with penicillin or carbenicillin as a carbon source and were found to be extensively antibiotic resistant¹⁵. To confirm the stability of the antibiotic catabolism phenotypes after extended storage at -80°C , and to control for the unlikely possibility that growth in previous studies was affected by trace amounts of EDTA, we cultured each strain with aeration in M9 media containing 0 g/L, 0.25 g/L, 0.5 g/L, or 1 g/L penicillin as the sole carbon source at 25°C and measured culture density over the course of 1 week (Fig. 1). Each strain grew in a dose-dependent manner, with 1 g/L penicillin supporting the most robust growth.

¹Department of Pathology and Immunology, Washington University in St Louis School of Medicine, Saint Louis, MO, USA. ²The Edison Family Center for Genome Sciences and Systems Biology, Washington University in St Louis School of Medicine, Saint Louis, MO, USA. ³Wyss Institute for Biologically Inspired Engineering, Harvard, Cambridge, MA, USA. ⁴US Army Edgewood Chemical Biological Center, Aberdeen Proving Ground, Aberdeen, MD, USA.

⁵Novo Nordisk Foundation Center for Biosustainability, Technical University of Denmark, Lyngby, Denmark. ⁶Department of Molecular Microbiology, Washington University in St Louis School of Medicine, Saint Louis, MO, USA. ⁷Department of Biomedical Engineering, Washington University in St Louis, Saint Louis, MO, USA. ⁸Present address: Division of Basic Sciences, Fred Hutchinson Cancer Center, Seattle, WA, USA. ⁹Present address: TMG Biosciences, LLC, Austin, TX, USA. ¹⁰Deceased. *e-mail: dantas@wustl.edu

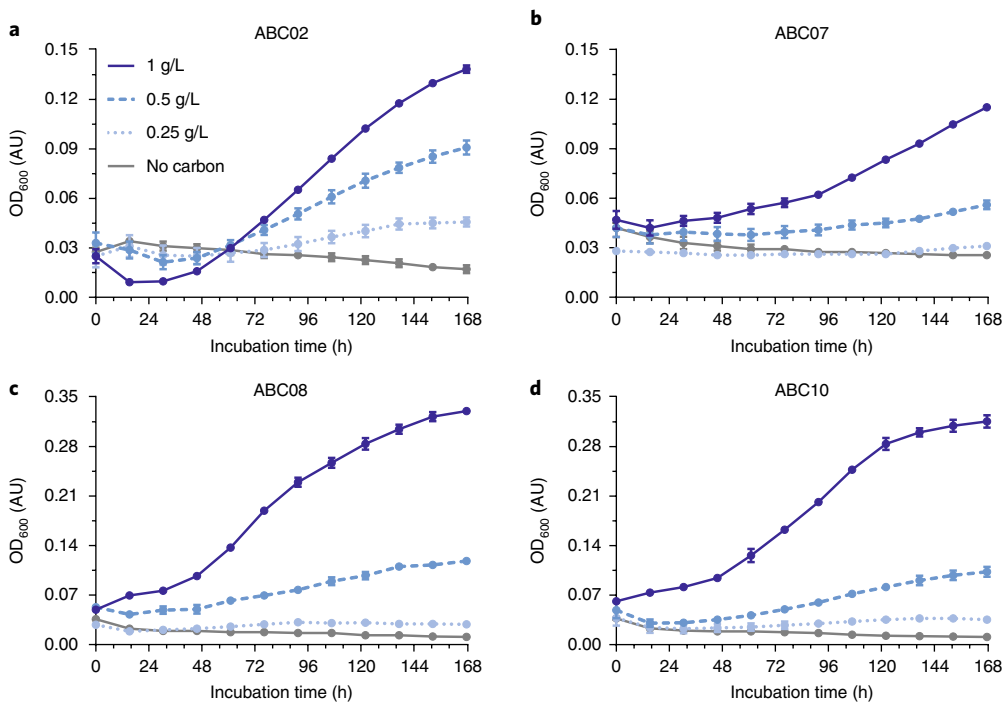


Fig. 1 | ABC strains catabolize penicillin as their sole carbon source. a–d, Growth of strains ABC02 (a), ABC07 (b), ABC08 (c), and ABC10 (d) in minimal media with penicillin as sole carbon source. Legend for penicillin carbon source concentration in a applies to all panels. Data points are average of three experiments with s.e.m. error bars. OD₆₀₀, optical density at 600 nm.

ABC strains share penicillin-responsive gene regulation. To elucidate the enzymes and pathways used during penicillin catabolism, we annotated draft genomes²¹ from all four β -lactam catabolizing strains. In all four genomes we annotated multiple chromosomal β -lactamase genes, including genes annotated as belonging to class A, class C, and class D β -lactamase families (Supplementary Table 2), as well as complete or near-complete phenylacetic acid catabolic pathways^{22,23}. The four ABC strains are able to grow in rich media in the presence of high concentrations (1 g/L) of a variety of β -lactam antibiotics including penicillins (all four ABC strains), cephalosporins (ABC07, ABC08, and ABC10), monobactams (ABC02, ABC08, and ABC10), and, to a limited extent, carbapenems (ABC07, ABC08, and ABC10) (Supplementary Fig. 1).

These findings led us to hypothesize that catabolism of penicillin proceeds through canonical hydrolysis of the β -lactam ring to produce benzylpenicilloic acid^{24,25}, which is then processed downstream to central metabolism. We tested this hypothesis using a comparative transcriptomic approach, wherein the four ABC strains were independently cultured in minimal media with a variety of single-carbon sources, and their whole-cell gene expression levels were measured and compared under these conditions via RNA-seq. To choose substrates with known paths to central metabolism, we initially tested the ability of each of the four strains to utilize 190 distinct carbon sources in a high-throughput phenotypic microarray assay. Each strain grew on a unique subset of carbon sources (Supplementary Fig. 2), and each strain was cultured with penicillin or a carbon source that feeds directly into central metabolism (glucose for ABC07 and histidine for ABC02, ABC08, and ABC10). Following RNA-seq, we analyzed the transcriptome for differentially expressed genes under these two conditions (see Supplementary Dataset 1 for counts and heat map representation of data). Remarkably, the RNA-seq data suggest that all four strains may utilize a conserved strategy for antibiotic catabolism, consisting of upregulation of Ambler class A, C, and D β -lactamases²³ (Supplementary Table 3), amidases (syntetic with a β -lactamase in

strains ABC07, ABC08, and ABC10), and genes involved in phenylacetic acid utilization (Fig. 2a). Interestingly, in the phenotypic microarray assay, all four strains showed robust growth on aromatic substrates, especially phenylalanine and derivatives of phenylacetic acid (Supplementary Fig. 2).

Notably, the side chain of penicillin (the non- β -lactam region) consists of phenylacetamide, suggesting that growth on penicillin in the ABC strains might proceed through metabolism of this part of the molecule. To test this proposal, we performed additional RNA-seq experiments with the *Pseudomonas* strain ABC07 grown on benzylpenicilloic acid (the product of β -lactamase cleavage of penicillin) or phenylacetic acid as the sole carbon source, in addition to penicillin and glucose as before (Fig. 2b). These data reveal an apparent transcriptional architecture, beginning with a β -lactamase being preferentially upregulated in response to penicillin (compared to glucose: ~65-fold with an adjusted *P* value of 1.6×10^{-91}). This is followed by expression of a putative penicillin utilization operon (*put*) consisting of four open reading frames that appear to be responsive to both penicillin and benzylpenicilloic acid, but not phenylacetic acid: a β -lactamase (~6-fold with an adjusted *P* value of 2.2×10^{-8} compared to glucose), a major facilitator family importer (~122-fold with an adjusted *P* value of 2.5×10^{-128} compared to glucose), and two amidases (termed *put1* and *put2* here; respectively, ~122-fold with an adjusted *P* value of 1.3×10^{-131} and ~240-fold with an adjusted *P* value of 1.0×10^{-126} compared to glucose). Finally, the pathway is apparently completed by upregulation of the phenylacetic acid catabolism (*paa*) in response to penicillin, benzylpenicilloic acid, and phenylacetic acid (Fig. 2b). This architecture suggests a conserved catabolic pathway consisting of the following steps: (i) detoxification of penicillin via hydrolysis of the β -lactam ring by a β -lactamase, a canonical β -lactam antibiotic resistance enzyme, (ii) import of the benzylpenicilloic acid product and/or hydrolysis of the amide bond to free the carbon-rich phenylacetic acid side chain, and (iii) processing of phenylacetic acid into acetyl-CoA and succinyl-CoA via the phenylacetic acid catabolism (Fig. 2c).

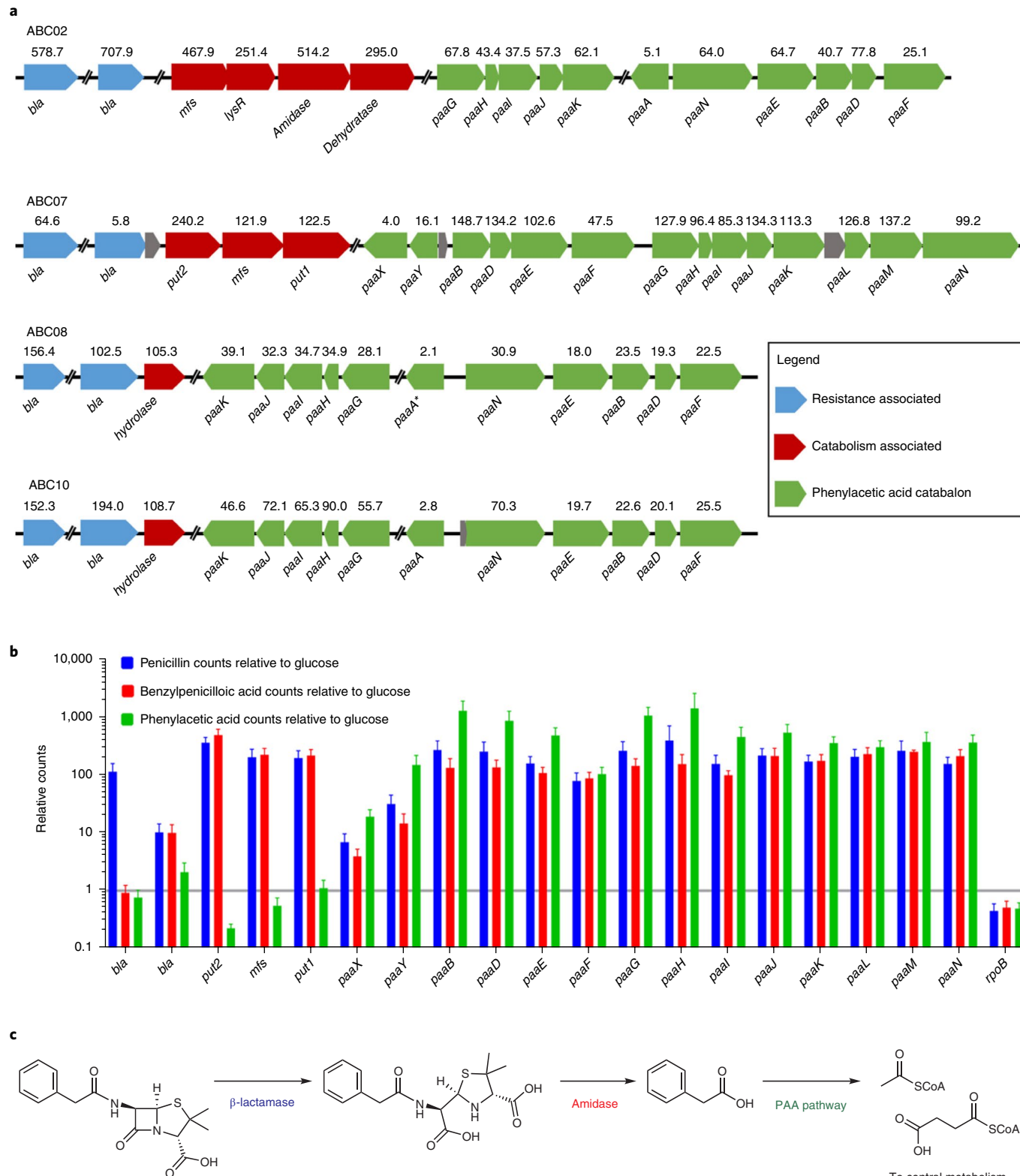


Fig. 2 | Evidence for shared strategy for penicillin catabolism among ABC strains. **a**, Upregulated open reading frames (ORFs) during growth on penicillin compared to histidine (all but ABC07) or glucose (ABC07) calculated from triplicate cultures. Displayed above each ORF is the relative fold upregulation and below is the gene name (*bla*, β -lactamase; *mfs*, major facilitator superfamily pump). All genes displayed showed significant upregulation at adjusted P value < 0.00001 (DESeq) except for *paaA* of ABC08. **b**, ABC07 transcriptional response to penicillin, benzylpenicilloic acid, and phenylacetic acid relative to glucose. Relative transcript counts of ORFs identified as responsive to penicillin are displayed as averages of triplicate RNA-seq experiments with s.e.m. error bars. The housekeeping RNA polymerase gene *rpoB* is present for comparison. **c**, Hypothesized pathway for penicillin degradation. Penicillin is neutralized by a β -lactamase to produce benzylpenicilloic acid, which acts as substrate for amidases or other hydrolases, releasing phenylacetic acid which is routed to central metabolism as a carbon source by the phenylacetic acid catabalon.

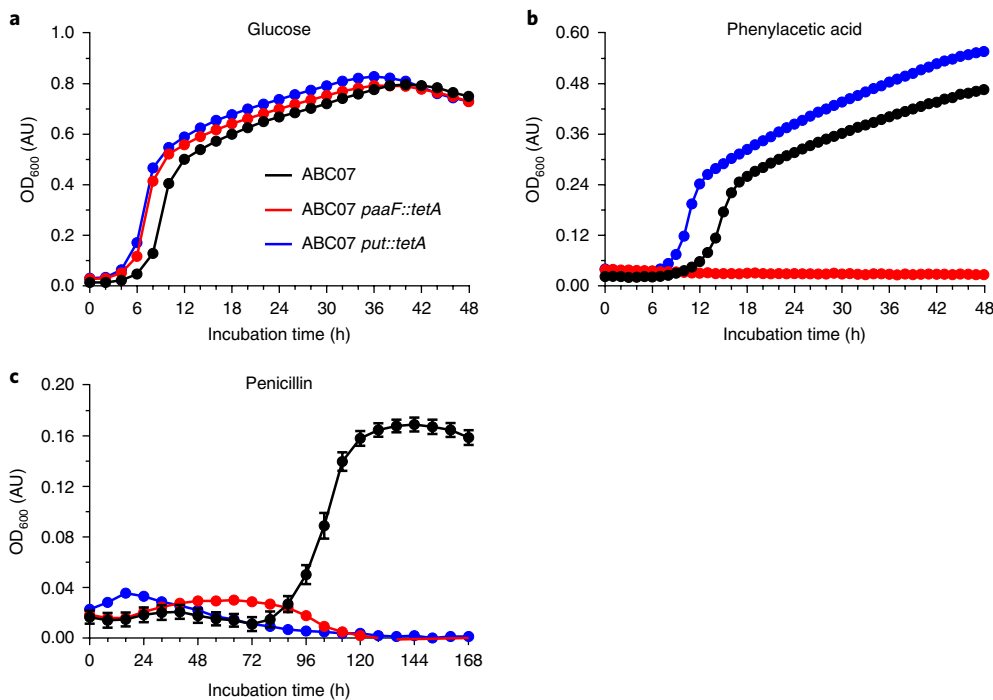


Fig. 3 | paaF and the put operon are necessary for penicillin catabolism in ABC07. **a–c,** Growth curves of wild-type ABC07 (black), paaF::tetA (red) and put::tetA (blue) strains in minimal media containing glucose (**a**), phenylacetic acid (**b**), or penicillin (**c**) as the sole carbon source. Measurements are the average of triplicate cultures with s.e.m. displayed.

Growth on penicillin requires paa and put operons. To determine the necessity for the phenylacetic acid catabolism and the *put* operon in strain ABC07 (Fig. 2), we constructed knockout strains of ABC07 in which the *paaF* gene (phenylacetyl-CoA ligase, responsible for the first step of phenylacetic acid catabolism²²) and the entire *put* operon (consisting of a β -lactamase, *put2*, *mfs*, and *put1*) were each replaced chromosomally²⁶ with a *tetA* open reading frame. These strains, alongside wild-type ABC07, were assayed for their ability to grow in M9 media with 0.4% glucose, phenylacetic acid, or penicillin as their sole carbon source. In support of our hypothesis, loss of *paaF* resulted in a strain that, while still able to grow well with glucose (Fig. 3a), was no longer able to sustain growth on phenylacetic acid (Fig. 3b). More interestingly, the *paaF* strain also showed lack of growth using penicillin as sole carbon source, indicating that penicillin catabolism flows through phenylacetic acid (Fig. 3c). Contrasting this is the phenotype of the *put* knockout, which can grow using either glucose or phenylacetic acid as its carbon source (Fig. 3a,b), indicating little, if any, role for these four genes in central metabolism or growth on aromatic substrates. Notably, though, loss of the *put* operon resulted in complete loss of penicillin catabolism (Fig. 3c), indicating the necessity of these genes, along with the *paa* catabolism, for the antibiotic catabolism phenotype.

Catabolism of the phenylacetamide side chain. Because we found ABC07 to be resistant to a variety of additional β -lactam antibiotics at 1 g/L (Supplementary Fig. 1), we next tested the ability of these compounds, as well as penicillin degradation products, to support growth of ABC07 strains in M9 media as carbon sources at 1 g/L (Supplementary Fig. 3). Of the new carbon sources tested, only one—benzylpenicilloic acid—supported the growth of ABC07, but neither the *paaF* nor the *put* mutants were capable of growth using it as a sole carbon source (Supplementary Fig. 3b), mirroring our observations with penicillin (Fig. 3c and Supplementary Fig. 3a). Interestingly, whereas phenylacetic acid supports growth of ABC07 and the *put* strain (Fig. 3b and Supplementary Fig. 3c), the

other half of the penicillin structure, the 6-aminopenicillanic acid β -lactam core, does not (Supplementary Fig. 3d), supporting the hypothesis that in ABC07 penicillin catabolism runs almost solely through the phenylacetamide side chain. Further reinforcing this is our observation that none of the ABC07 strains are capable of growth using other β -lactam antibiotics, including other penicillin-class drugs (carbenicillin or ampicillin, Supplementary Fig. 3e,f) or the cephalosporin cefuroxime (Supplementary Fig. 3g).

The put operon includes a benzylpenicilloic acid amidase. The presence of amidases and hydrolases that are upregulated by penicillin and benzylpenicilloic acid may suggest the involvement of penicillin amidase (also known as penicillin acylase) enzymes from the N-terminal nucleophile hydrolase enzyme family that are used industrially to hydrolyze the phenylacetamide side chain of penicillin from the β -lactam ring to produce 6-aminopenicillanic acid in the manufacture of semisynthetic β -lactam antibiotics²⁷. We constructed a phylogenetic tree using the ABC strain amidase and hydrolase sequences, their nearest neighbors in NCBI's NR database²⁸, and canonical penicillin amidases (EC 3.5.11) downloaded from UniProt²⁹ (Supplementary Fig. 4). The ABC proteins do not appear to cluster with the canonical penicillin amidases and instead group with amidases, amidohydrolases, or hydrolases of unknown specificity (Supplementary Fig. 4).

Because of their limited annotation, catabolic necessity in ABC07 (Fig. 3 and Supplementary Fig. 3), and transcriptional response to penicillin and benzylpenicilloic acid (Fig. 2b), we chose to study the gene products of *put1* and *put2* in greater detail following heterologous expression in *E. coli* and purification (Supplementary Fig. 5a). We assayed the resulting purified enzymes for amidase activity by incubation with two chromogenic amide substrates: 6-nitro-3-(phenylacetamido)-benzoic acid (NIPAB) and *p*-nitroacetanilide. Both substrates have previously been validated as model chromogenic substrates for penicillin³⁰ (NIPAB) or generic amides³¹ (*p*-nitroacetanilide). For comparison, we also carried out

reactions using a commercially available *E. coli* penicillin amidase enzyme. We found Put1 and Put2 to be functionally distinct from penicillin amidase in their inability to hydrolyze the amide bond in NIPAB while showing activity with *p*-nitroacetanilide, with penicillin amidase demonstrating the opposite activities (Supplementary Fig. 5b,c). Notably, hydrolysis of the amide bonds in these molecules is functionally equivalent to the hydrolysis of the amide bonds found in penicillin or benzylpenicilloic acid that would result in release of phenylacetic acid.

We next compared the Michaelis–Menten dynamics of Put1, because of its apparent greater activity, as well as penicillin amidase across four additional substrates including another penicillin analog³² (Supplementary Fig. 5d) and three potential peptidase substrates (Supplementary Fig. 5e–g). These assays reveal limited functional overlap between *E. coli* penicillin amidase and Put1. We therefore undertook a more detailed bioinformatic examination of Put1 in comparison to penicillin amidases. Analysis of the amino acid sequence of Put1 suggests that it lacks a signal peptide found in many penicillin amidases, and Put1 similarly lacks two critical active site residues found in penicillin amidase and N-terminal nucleophile hydrolase family enzymes: a catalytic serine/threonine/cysteine and an asparagine residue in the oxyanion hole^{33–35} (Supplementary Fig. 6a). Because structure can sometimes more accurately predict enzyme classification than sequence alone (notably in the case of β -lactamases³³), we compared the predicted homology-based three-dimensional structure of Put1 to the published crystal structure of *E. coli* penicillin amidase. Although the alignment of Put1 to *E. coli* penicillin amidase reveals no substantial overlap (Supplementary Fig. 6b), a comparison of the alignment of three authentic penicillin amidase structures shows notable conservation (Supplementary Fig. 6c). Together, these findings indicate that Put1 is not a penicillin amidase and is instead likely an amidase with nonspecific activity.

To directly evaluate the ability of Put1 to hydrolyze penicillin or benzylpenicilloic acid as opposed to using chromogenic analogs (Supplementary Fig. 5), we developed a pH-shift kinetic assay³⁶ to compensate for the fact that these two substrates show limited spectroscopic changes during hydrolysis and are, in effect, invisible substrates. Whereas other methods for measuring β -lactam hydrolysis rely on specialized instruments such as pH-stat titrators^{37,38} or indirect measurement and complex modeling using chromogenic competing substrates³⁹, the pH-shift assay can be monitored on a standard UV visible (UV–Vis) spectrometer and is directly linked to substrate conversion. Using this assay, we verified that *E. coli* penicillin amidase and commercial *B. cereus* β -lactamase enzymes both exhibit Michaelis–Menten kinetics with penicillin as a substrate, as expected. However, we did not observe any substantial activity during incubation of Put1 with penicillin (Fig. 4a), nor did a follow-up liquid chromatography tandem mass spectrometry (LC–MS) assay detect any substantial loss of penicillin in a separate reaction (Supplementary Fig. 7a). Notably, the hydrolysis of either the phenylacetamide or β -lactam bonds in penicillin would result in formation of a carboxylic acid and a change in signal in the pH-shift assay. In contrast, when both Put1 and *E. coli* penicillin amidase were incubated with benzylpenicilloic acid as a substrate, we observed Michaelis–Menten kinetics (Fig. 4b). Though the kinetics observed for penicillin amidase and β -lactamase with penicillin could represent the hydrolysis of either the phenylacetamido or the β -lactam amide bonds, the only amide bond present in benzylpenicilloic acid is that of the phenylacetamido group, as the β -lactam amide bond is already hydrolyzed. An orthologous assay using the fluorescent derivatization reagent NBD-Cl similarly detected that a new amino group⁴⁰ is revealed during incubation of Put1 with benzylpenicilloic acid, but not penicillin (Supplementary Fig. 7b). These results are consistent with the hydrolysis of benzylpenicilloic acid to form phenylacetic acid. The lack of activity of Put1 with penicillin

further supports our hypothesis that Put1 acts downstream of a β -lactamase.

Finally, we directly confirmed hydrolysis of benzylpenicilloic acid by Put1 using LC–MS. In vitro reactions containing benzylpenicilloic acid and no enzyme, Put1, or penicillin amidase were quenched at three time points and analyzed for loss of benzylpenicilloic acid (Fig. 4c; the reaction product, phenylacetic acid, is not detectable by this LC–MS method). The Put1 reactions showed substantial benzylpenicilloic acid elimination (Fig. 4c,d), confirming the hydrolysis that was indicated in the pH-shift (Fig. 4b) and NBD-Cl assays (Supplementary Fig. 7b). These results are in concordance with our hypothesized penicillin catabolic pathway in ABC07, with Put1 acting on benzylpenicilloic acid rather than penicillin, and may also explain the phenotypic and transcriptional data from ABC02, ABC08, and ABC10 (Fig. 2a). In this pathway, the canonical β -lactamase antibiotic resistance enzyme inactivates penicillin to produce benzylpenicilloic acid, which in turn acts as substrate for promiscuous amidase enzymes such as Put1. This results in the release of phenylacetic acid, which is processed by the *paa* catabolon to produce acetyl-CoA and succinyl-CoA, which feed into central metabolism.

***E. coli* expressing *put* operon catabolizes penicillinoids.** Based on our characterization of the β -lactam catabolic pathways of four soil bacteria, it appears that subsistence on penicillin as a carbon source requires penicillin resistance through β -lactamase activity, the *paa* catabolon, and an amidase to link these two functions metabolically (Fig. 2c). We set out to test this hypothesis first by engineering an *E. coli* strain to use penicillin as its sole carbon source. We selected the strain *E. coli* W (ATCC 9637) because of the presence of a complete and functional *paa* catabolon in this lineage⁴¹ and its use industrially as a source of penicillin amidase²⁷. We confirmed the ability of this strain to catabolize phenylacetic acid in M9 media and cloned an *E. coli* penicillin amidase gene (*pga*)⁴² with truncated signal peptide (which is necessary due to toxicity issues under constitutive expression) into a β -lactamase-expressing vector. We found that carriage of this plasmid was sufficient to confer the ability to subsist on penicillin as a sole carbon source in a dose-dependent manner (Fig. 5a). Although the *pga* gene expressed on the vector originates from the *E. coli* W chromosome, chromosomal expression is insufficient for allowing growth during the time frame investigated, as demonstrated by the lack of growth by the vector control strain (Fig. 5a). The importance of amidase activity for penicillin catabolism is further underscored by the loss of this phenotype in the *pga*-overexpression strain during growth at 37 °C rather than at 28 °C as a result of the inhibition of penicillin amidase post-translational modifications at 37 °C²⁷ (Fig. 5b). This experiment demonstrates the potential utility of engineering bacteria for bioremediation of antibiotics.

With this proof of principle in hand, we set out to test the ability of the *put* operon to confer increased penicillinoid (i.e., penicillin and its degradation products) catabolism. When expressed in *E. coli* W, the *put* operon was not sufficient to give substantially better growth on penicillin compared to vector controls. This is perhaps unsurprising, as penicillin catabolism in ABC07 requires greater than 100-fold overexpression of the *put* operon (Fig. 2a,b), presumably to augment the low nonspecific amidase activity, and it is unclear how levels reached in *E. coli* might compare. Furthermore, during purification of Put1 from heterologous expression in *E. coli*, we found that this enzyme in particular shows limited stability, with the bulk of the enzyme localizing to the insoluble fraction of cell extracts (Supplementary Fig. 8), indicating poor solubility and compatibility in *E. coli*. However, we did observe that benzylpenicilloic acid as a carbon source can support growth in the *pga*-overexpressing *E. coli* strain and that this growth occurs after a shorter lag phase compared to growth on penicillin (Fig. 5a,c).

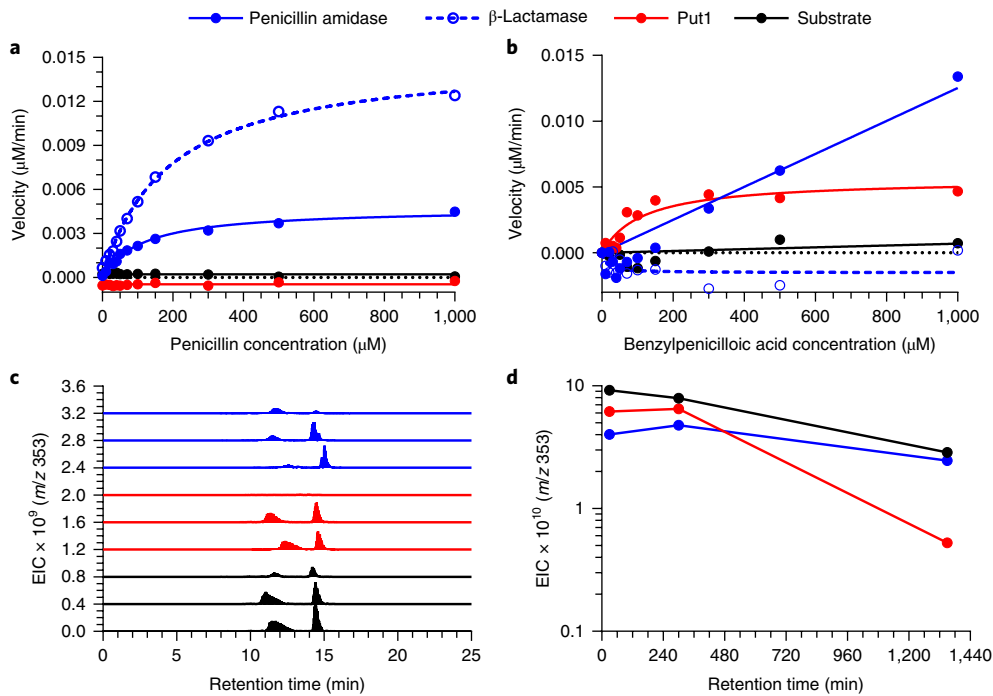


Fig. 4 | Put1 is a benzylpenicilloic-acid-hydrolyzing amidase. **a,b**, Hydrolysis activity of *E. coli* penicillin amidase, *B. cereus* β-lactamase, and Put1 with penicillin (**a**) or benzylpenicilloic acid (**b**) as a substrate was assayed by monitoring absorbance at 404 nm with the colorimetric pH indicators *p*-nitrophenol and *m*-nitrophenol, respectively. **c**, LC-MS analysis of benzylpenicilloic acid degradation by *E. coli* penicillin amidase or Put1 by extracted ion count monitoring. 353 *m/z* corresponds to singly protonated benzylpenicilloic acid. Within each condition, traces represent (bottom to top) incubation for 30 min, 300 min, and 22.5 h. Note, benzylpenicilloic acid spontaneously equilibrates to form two diastereomers in aqueous solutions. **d**, Time course of reactions in **c** measured by 353 *m/z* total ion count.

When we assayed growth of both engineered *E. coli* strains using benzylpenicilloic acid as a carbon source, we found that expression of the *put* operon was sufficient to confer a significant improvement in growth compared to its vector control measured both by lag time (Fig. 5c) and culture-density reached (Fig. 5d). These results confirm the validity of our hypothesized pathway, as well as a role for the *put* operon in this pathway.

Discussion

Here we describe the first characterization of an antibiotic catabolism pathway and find that it relies on a novel amidase activity to link β-lactamase and phenylacetic acid catabolism activities (Fig. 2). In strain ABC07, a penicillin utilization operon, *put*, is regulated by penicillin and its β-lactamase product benzylpenicilloic acid (Fig. 2b) and is necessary for growth on penicillin alongside the phenylacetic acid catabolon (Fig. 3 and Supplementary Fig. 3). The *put* operon encodes an enzyme with promiscuous amidase activity (Supplementary Fig. 5) that degrades benzylpenicilloic acid via hydrolysis of the amide bond (Fig. 4b–d and Supplementary Fig. 7b). We applied this knowledge to design two strains of *E. coli* that can consume penicillin as a sole carbon source (Fig. 5). These results led us to develop two related models for penicillin catabolism in bacteria (Fig. 6). The first model (Fig. 6a) describes our hypothesis for penicillin catabolism in strain ABC07. In this model, penicillin enters the periplasm through outer-membrane porins, where the β-lactam ring is hydrolyzed by β-lactamases to produce benzylpenicilloic acid. Both Put1 and Put2 lack predicted secretion signals⁴³ and are likely localized to the cytoplasm, where they can hydrolyze the amide bond of benzylpenicilloic acid to produce phenylacetic acid and penicic acid. Because there are no known benzylpenicilloic acid inner-membrane transporters, we propose that in ABC07 the MFS import pump located in the *put* operon

(Fig. 2a) may fulfill this role. Finally, phenylacetic acid feeds into central metabolism through the phenylacetic acid catabolon. In our second model (Fig. 6b) we propose a modified route for penicillin catabolism in our engineered *E. coli* strain. In this model, both β-lactamase and penicillin amidase are secreted into the periplasm, where phenylacetic acid is produced by penicillin amidase, either from penicillin or from benzylpenicilloic acid. In this model, transport of phenylacetic acid into the cytoplasm is mediated by the Paal permease, part of the phenylacetic acid catabolon.

These two models differ in their requirements for a β-lactamase enzyme. In the *pga*-overexpressing *E. coli* model, the β-lactamase acts as a resistance gene only, as *E. coli* penicillin amidase can use either penicillin or benzylpenicilloic acid as a substrate (Fig. 4 and Supplementary Fig. 7a; see also refs^{8,38}). In this case, resistance and catabolism could theoretically be decoupled through alternative means of resistance. In contrast, Put1 appears to act only on benzylpenicilloic acid (Fig. 4 and Supplementary Fig. 7) such that in ABC07, and potentially other antibiotic consuming bacteria, β-lactamases may act bifunctionally in resistance and catabolism pathways. This theory is supported by the presence of penicillin-responsive β-lactamases syntetic to amidases and hydrolases on the chromosomes of ABC07, ABC08, and ABC10 (Fig. 2a). Based on its slow kinetics, it does not appear that Put1 uses penicillin or benzylpenicilloic acid as its natural substrate (Fig. 4b), but the proximity of the *put1* and *put2* genes to a β-lactamase gene may allow them to be sufficiently upregulated in the presence of penicillin (Fig. 2b) to overcome catalytic inefficiencies. Notably, because they do not act on penicillin, the low catalytic efficiency of Put1 and Put2 does not endanger the host cell, as they are not called upon to act as resistance genes. Synteny of β-lactamases with amidases may therefore present an advantageous pre-condition for penicillin catabolism in the context of a genome containing a phenylacetic acid catabolic

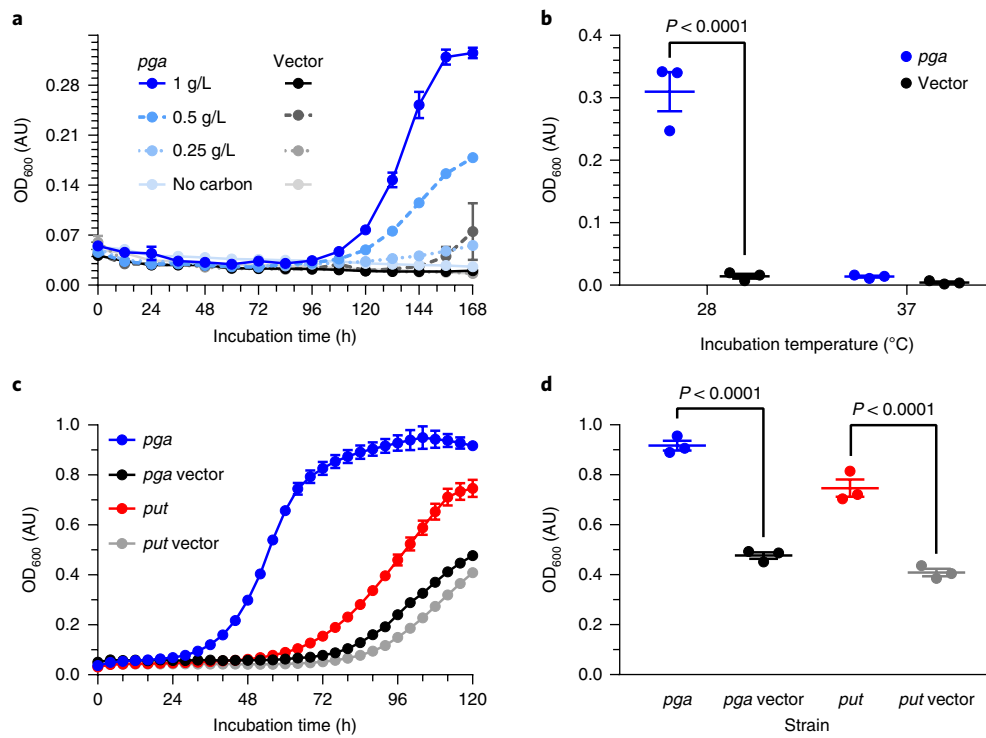


Fig. 5 | *E. coli* expression of penicillin amidase or the *put* operon gives significantly increased growth on penicillinoids. a, Growth curve of *E. coli* W in minimal media with β -lactamase and penicillin amidase (*pga*, blue traces) expression or vector β -lactamase expression only (black traces) with penicillin as the sole carbon source. **b**, Final culture densities of *E. coli* W expressing β -lactamase and penicillin amidase (*pga*, blue) or β -lactamase only (black) grown at 28 °C vs. 37 °C in minimal media with penicillin as sole carbon source. **c**, Growth curves of *E. coli* W expressing penicillin amidase (*pga*) or vector control (blue and black lines, respectively) or *put* operon or vector controls (red and gray lines, respectively) in minimal media with benzylpenicilloic acid as sole carbon source. **d**, Final culture OD₆₀₀ values of *E. coli* W expressing penicillin amidase (*pga*) or vector control (blue and black, respectively) or *put* operon or vector control (red and gray, respectively). Significance was determined by pair-wise ANOVA with Bonferroni correction. All data points are average of triplicate cultures with s.e.m. error shown.

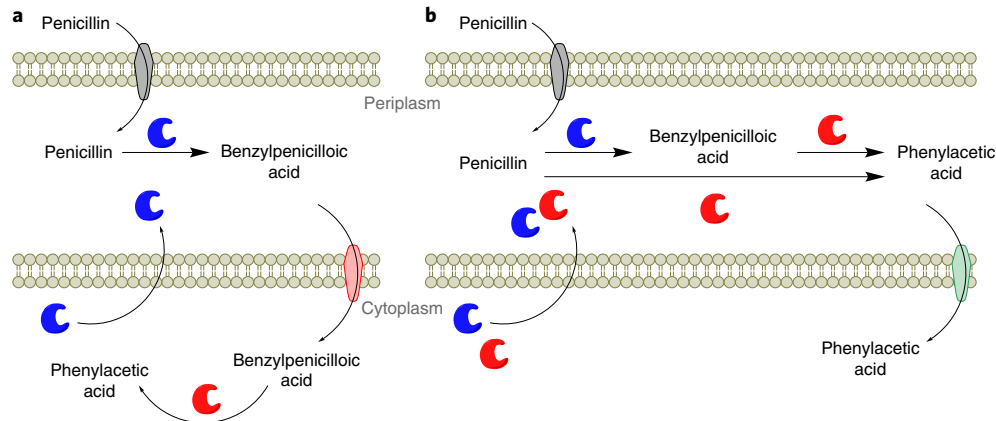


Fig. 6 | Schematics illustrating penicillin catabolic strategies. a, Hypothesized mechanism of penicillin catabolism in ABC07 and studied ABC strains. Outer-membrane porins (gray membrane protein) allow uptake of penicillin to the periplasm. In the periplasm, β -lactamases (blue enzyme) rapidly detoxify penicillin to benzylpenicilloic acid. MFS pumps (red membrane protein) transport benzylpenicilloic acid to the cytoplasm, where amidases (for example, Put1, red enzyme) hydrolyze the amide bond to release the phenylacetic acid carbon source. **b**, Hypothesized mechanism of penicillin catabolism in engineered *E. coli*. Similar to **a**, with amide hydrolysis of penicillin or benzylpenicilloic acid occurring in the periplasm via secreted penicillin amidase (red enzyme), and transport of phenylacetic acid to the cytoplasm occurring via Paal phenylacetic acid permease (green membrane protein).

pathway. We therefore searched the local genomic context of a library of functionally validated β -lactamase genes for the presence of amidases or genes with related functions. Our analysis found that 2.5% of β -lactamase genes are syntenic (within *ca.* 1.5 kb) to potential amidases. These pairings fulfill two of three conditions hypoth-

esized in our model for ABC07 (Fig. 6a). A recent genome survey has found that the phenylacetic acid catabolite is present in ~16% of genomes²², implying that the coincidence of all three conditions likely occurs in the soil and that the penicillin-catabolizing phenotype is far from limited to the four strains analyzed. We propose that

antibiotic inactivation followed by carbon-source release through a promiscuous enzyme is likely employed by soil bacteria catabolizing other antibiotics as well. We predict that ongoing and future studies will shed further light on these activities.

Antibiotic resistance enzymes are known to be plentiful in soil habitats³, and it is only because of their medical exploitation that antibiotics are treated as privileged molecules not bound by the carbon cycle. Here we have provided ample evidence for the normality of antibiotics in this regard. We characterize a complete antibiotic catabolic pathway that uniquely provides a mechanistic connection between antibiotic producers, antibiotic resistance, and antibiotic catabolism. We have leveraged this mechanistic understanding to engineer *E. coli* strains that can catabolize penicillin and its degradation product as a sole carbon source. With limited further engineering, these strains could be developed as tools for in situ bioremediation of antibiotic-contaminated soils or environments, such as those located near pharmaceutical manufacturers⁴⁴. These environments are important drivers of antibiotic resistance development⁴⁵, and their remediation could help prevent the spread of resistance. Of course, the benefits of any such bioremediation program would need to be weighed against the risk of releasing a genetically modified bacterium into the environment and the potential spread of antibiotic resistance/degradation genes to other organisms. Finally, antibiotic-catabolizing enzymes have the potential to play an important industrial role in the production of next-generation antibiotics in the same way that the discovery of penicillin amidase spurred the development of semisynthetic β -lactams through remodeling of natural penicillins. Characterization of hydrolytic enzymes responsible for the catabolism of other antibiotics, such as hypothetical glycosidases acting on aminoglycosides¹⁶, could catalyze an explosion of diverse semisynthetic derivatives in other antibiotic classes. Antibiotic degradation may therefore paradoxically contribute to the development of the next generation of novel antibiotics.

Methods

Methods, including statements of data availability and any associated accession codes and references, are available at <https://doi.org/10.1038/s41589-018-0052-1>.

Received: 3 August 2017; Accepted: 8 March 2018;

Published online: 30 April 2018

References

- Davies, J. & Davies, D. Origins and evolution of antibiotic resistance. *Microbiol. Mol. Biol. Rev.* **74**, 417–433 (2010).
- D'Costa, V. M. et al. Antibiotic resistance is ancient. *Nature* **477**, 457–461 (2011).
- Crofts, T. S., Gasparrini, A. J. & Dantas, G. Next-generation approaches to understand and combat the antibiotic resistome. *Nat. Rev. Microbiol.* **15**, 422–434 (2017).
- Forsberg, K. J. et al. The shared antibiotic resistome of soil bacteria and human pathogens. *Science* **337**, 1107–1111 (2012).
- Aust, M.-O. et al. Distribution of sulfamethazine, chlortetracycline and tylosin in manure and soil of Canadian feedlots after subtherapeutic use in cattle. *Environ. Pollut.* **156**, 1243–1251 (2008).
- Wright, P. M., Seiple, I. B. & Myers, A. G. The evolving role of chemical synthesis in antibacterial drug discovery. *Angew. Chem. Int. Ed. Engl.* **53**, 8840–8869 (2014).
- Pramer, D. & Starkey, R. L. Decomposition of streptomycin. *Science* **113**, 127 (1951).
- Kameda, Y., Kimura, Y., Toyoura, E. & Omori, T. A method for isolating bacteria capable of producing 6-aminopenicillanic acid from benzylpenillin. *Nature* **191**, 1122–1123 (1961).
- Abd-El-Malek, Y., Monib, M. & Hazem, A. Chloramphenicol, a simultaneous carbon and nitrogen source for a *Streptomyces* sp. from Egyptian soil. *Nature* **189**, 775–776 (1961).
- Johnsen, J. Utilization of benzylpenillin as carbon, nitrogen and energy source by a *Pseudomonas fluorescens* strain. *Arch. Microbiol.* **115**, 271–275 (1977).
- Beckman, W. & Lessie, T. G. Response of *Pseudomonas cepacia* to β -Lactam antibiotics: utilization of penicillin G as the carbon source. *J. Bacteriol.* **140**, 1126–1128 (1979).
- Johnsen, J. Presence of β -lactamase and penicillin acylase in a *Pseudomonas* sp. utilizing benzylpenillin as a carbon source. *J. Gen. Appl. Microbiol.* **27**, 499–503 (1981).
- Wang, P. et al. Characterization and mechanism analysis of penicillin G biodegradation with *Klebsiella pneumoniae* Z1 isolated from waste penicillin bacterial residue. *J. Ind. Eng. Chem.* **27**, 50–58 (2015).
- Barnhill, A. E., Weeks, K. E., Xiong, N., Day, T. A. & Carlson, S. A. Identification of multiresistant *Salmonella* isolates capable of subsisting on antibiotics. *Appl. Environ. Microbiol.* **76**, 2678–2680 (2010).
- Dantas, G., Sommer, M. O. A., Oluwasegun, R. D. & Church, G. M. Bacteria subsisting on antibiotics. *Science* **320**, 100–103 (2008).
- Bello González, Tde.J., Zuidema, T., Bor, G., Smidt, H. & van Passel, M. W. Study of the aminoglycoside subsistence phenotype of bacteria residing in the gut of humans and zoo animals. *Front. Microbiol.* **6**, 1550 (2016).
- Xin, Z. et al. Isolation, identification and characterization of human intestinal bacteria with the ability to utilize chloramphenicol as the sole source of carbon and energy. *FEMS Microbiol. Ecol.* **82**, 703–712 (2012).
- Topp, E. et al. Accelerated biodegradation of veterinary antibiotics in agricultural soil following long-term exposure, and isolation of a sulfamethazine-degrading sp. *J. Environ. Qual.* **42**, 173–178 (2013).
- Tappe, W. et al. Degradation of sulfadiazine by *Microbacterium lacus* strain SDZm4, isolated from lysimeters previously manured with slurry from sulfadiazine-medicated pigs. *Appl. Environ. Microbiol.* **79**, 2572–2577 (2013).
- Walsh, F., Amyes, S. G. B. & Duffy, B. Challenging the concept of bacteria subsisting on antibiotics. *Int. J. Antimicrob. Agents* **41**, 558–563 (2013).
- Crofts, T. S. et al. Draft genome sequences of three β -lactam-catabolizing soil *Proteobacteria*. *Genome Announc.* **5**, e00653–17 (2017).
- Teufel, R. et al. Bacterial phenylalanine and phenylacetate catabolic pathway revealed. *Proc. Natl Acad. Sci. USA* **107**, 14390–14395 (2010).
- Bush, K. & Jacoby, G. A. Updated functional classification of β -lactamases. *Antimicrob. Agents Chemother.* **54**, 969–976 (2010).
- Blair, J. M. A., Webber, M. A., Baylay, A. J., Ogbolu, D. O. & Piddock, L. J. V. Molecular mechanisms of antibiotic resistance. *Nat. Rev. Microbiol.* **13**, 42–51 (2015).
- Ghebre-Sellassie, I., Hem, S. L. & Knevel, A. M. Epimerization of benzylpenicilloic acid in alkaline media. *J. Pharm. Sci.* **73**, 125–128 (1984).
- Hmelo, L. R. et al. Precision-engineering the *Pseudomonas aeruginosa* genome with two-step allelic exchange. *Nat. Protoc.* **10**, 1820–1841 (2015).
- Valle, F., Balbás, P., Merino, E. & Bolívar, F. The role of penicillin amidases in nature and in industry. *Trends Biochem. Sci.* **16**, 36–40 (1991).
- Altschul, S. F. et al. Gapped BLAST and PSI-BLAST: a new generation of protein database search programs. *Nucleic Acids Res.* **25**, 3389–3402 (1997).
- UniProt Consortium. UniProt: a hub for protein information. *Nucleic Acids Res.* **43**, D204–D212 (2015).
- Svedas, V., Guranda, D., van Langen, L., van Rantwijk, F. & Sheldon, R. Kinetic study of penicillin acylase from *Alcaligenes faecalis*. *FEBS Lett.* **417**, 414–418 (1997).
- Hammond, P. M., Price, C. P. & Scawen, M. D. Purification and properties of aryl acylamidase from *Pseudomonas fluorescens* ATCC 39004. *Eur. J. Biochem.* **132**, 651–655 (1983).
- Szewczuk, A., Siewiński, M. & Słowińska, R. Colorimetric assay of penicillin amidase activity using phenylacetyl-aminobenzoic acid as substrate. *Anal. Biochem.* **103**, 166–169 (1980).
- Oinonen, C. & Rouvinen, J. Structural comparison of Ntn-hydrolases. *Protein Sci.* **9**, 2329–2337 (2000).
- McVey, C. E., Walsh, M. A., Dodson, G. G., Wilson, K. S. & Brannigan, J. A. Crystal structures of penicillin acylase enzyme-substrate complexes: structural insights into the catalytic mechanism. *J. Mol. Biol.* **313**, 139–150 (2001).
- McDonough, M. A., Klei, H. E. & Kelly, J. A. Crystal structure of penicillin G acylase from the Bro1 mutant strain of *Providencia rettgeri*. *Protein Sci.* **8**, 1971–1981 (1999).
- Janes, L. E., Löwendahl, A. C. & Kazlauskas, R. J. Quantitative screening of hydrolase libraries using pH indicators: identifying active and enantioselective hydrolases. *Chemistry* **4**, 2324–2331 (1998).
- Batchelor, F. R., Chain, E. B., Hardy, T. L., Mansford, K. R. & Rolinson, G. N. 6-Aminopenicillanic acid. III. Isolation and purification. *Proc. R. Soc. London. Ser. B, Biol. Sci.* **154**, 498–508 (1961).
- Margolin, A. L., Svedas, V. K. & Berezin, I. V. Substrate specificity of penicillin amidase from *E. coli*. *Biochim. Biophys. Acta* **616**, 283–289 (1980).
- Alkema, W. B., Floris, R. & Janssen, D. B. The use of chromogenic reference substrates for the kinetic analysis of penicillin acylases. *Anal. Biochem.* **275**, 47–53 (1999).
- Henke, E. & Bornscheuer, U. T. Fluorophoric assay for the high-throughput determination of amidase activity. *Anal. Chem.* **75**, 255–260 (2003).

41. Ferrández, A. et al. Catabolism of phenylacetic acid in *Escherichia coli*. Characterization of a new aerobic hybrid pathway. *J. Biol. Chem.* **273**, 25974–25986 (1998).
42. Schumacher, G., Sizmann, D., Haug, H., Buckel, P. & Böck, A. Penicillin acylase from *E. coli*: unique gene-protein relation. *Nucleic Acids Res.* **14**, 5713–5727 (1986).
43. Petersen, T. N., Brunak, S., von Heijne, G. & Nielsen, H. SignalP 4.0: discriminating signal peptides from transmembrane regions. *Nat. Methods* **8**, 785–786 (2011).
44. Larsson, D. G. J., de Pedro, C. & Paxeus, N. Effluent from drug manufactures contains extremely high levels of pharmaceuticals. *J. Hazard. Mater.* **148**, 751–755 (2007).
45. Pehrsson, E. C. et al. Interconnected microbiomes and resistomes in low-income human habitats. *Nature* **533**, 212–216 (2016).

Acknowledgements

This work is supported in part by awards to G.D. through the Edward Mallinckrodt, Jr. Foundation (Scholar Award), and from the NIH Director's New Innovator Award (<http://commonfund.nih.gov/newinnovator/>), the National Institute of Diabetes and Digestive and Kidney Diseases (NIDDK: <http://www.niddk.nih.gov/>), the National Institute of General Medical Sciences (NIGMS: <http://www.nigms.nih.gov/>), and the National Institute of Allergy and Infectious Diseases (NIAID: <https://www.niaid.nih.gov/>) of the National Institutes of Health (NIH) under award numbers DP2DK098089, R01GM099538, and R01AI123394, respectively. T.S.C. received support from a National Institute of Diabetes and Digestive and Kidney Diseases Training Grant through award number T32 DK077653 (P.I. Tarr, Principal Investigator) and a National Institute of Child Health and Development Training Grant through award number T32 HD049305 (K.H. Moley, Principal Investigator). K.J.F. received support from the NHGRI Genome Analysis Training Program (T32 HG00045), the NIGMS Cellular and Molecular Biology Training Program (T32 GM007067), and the NSF as a graduate research fellow (award number DGE-1143954). M.K.G. received support as a Mr. and Mrs. Spencer T.

Olin Fellow at Washington University and from the NSF as a graduate research fellow (DGE-1143954). Sequencing through the US Army Edgewood Chemical Biological Center was supported in part through funding provided by the Transformational Medical Technologies Initiative of the Defense Threat Reduction Agency, US Department of Defense. The content is solely the responsibility of the authors and does not necessarily represent the official views of the funding agencies. We are thankful to J. Hoisington-Lopez in the Center for Genome Sciences and Systems Biology at Washington University in St. Louis School of Medicine for Illumina sequencing support, T. Wencewicz and B. Evans for their useful discussions regarding biochemistry and LC–MS and members of the Dantas lab for general helpful discussions regarding the manuscript.

Author contributions

T.S.C., A.S., T.A.G., M.O.A.S., and G.D. conceived of experiments and design of work. T.S.C., B.W., A.S., and T.A.G. performed *in vitro*, microbial, and transcriptomic experiments. L.A.J., S.M.B., C.N.R., E.W.S., and H.S.G. sequenced strain genomes. T.S.C., A.S., T.A.G., K.J.F., and M.K.G. provided analyses. Article drafting was performed by T.S.C. with critical revision performed by T.S.C., B.W., A.S., K.J.F., M.K.G., M.O.A.S., and G.D.

Competing interests

The authors declare no competing interests.

Additional information

Supplementary information is available for this paper at <https://doi.org/10.1038/s41589-018-0052-1>.

Reprints and permissions information is available at www.nature.com/reprints.

Correspondence and requests for materials should be addressed to G.D.

Publisher's note: Springer Nature remains neutral with regard to jurisdictional claims in published maps and institutional affiliations.

Methods

Chemicals. For growth studies and enzymatic assays, high purity penicillin G sodium salt (Sigma, P3032), (+)-6-aminopenicillanic acid (Sigma, A70909), phenylacetic acid (Sigma, W287806), and other antibiotics were purchased. Dextro-(−)-benzylpenicilloic acid hydrate (Sigma, S341967) was purchased from the Sigma-Aldrich collection of rare and unique chemicals. *p*-Nitroacetanilide (Sigma, 130648), *p*-nitroaniline (Sigma, 185310), 6-nitro-3-(phenylacetamido) benzoic acid (aka NIPAB, Pfaltz and Bauer, N10625), *N*-phenylacetetyl-*p*-aminobenzoate (Sigma, P8529), L-glutamate 1-(*p*-nitroaniline) (Sigma, 49622), L-glutamate γ-(*p*-nitroaniline) (Sigma, G1135) and *N*α-benzoyl-DL-arginine *p*-nitroaniline (Sigma, B4875) were purchased as enzyme substrates and standards. For the kinetics assays *p*-nitrophenol (MP Biomedicals, 102461) and *m*-nitrophenol (Acros organics, 172300100) were purchased as indicators to monitor enzyme reaction kinetics in pH-shift assays. All other compounds and buffers used were of standard molecular biology grade.

Bacterial strains and growth conditions. Soil isolates and minimal media.

Soil isolates ABC02, ABC07, ABC08, and ABC10 were previously isolated by culturing with the antibiotics penicillin or carbenicillin as carbon sources and were maintained at −80 °C as 15% glycerol stocks in single carbon source (SCS) minimal media (SCS media, see below)¹⁵. Isolates were cultured with aeration (taken to be shaking at 220 r.p.m. throughout unless otherwise specified) at 22 °C in LB or M9 minimal media (M9 media, see below). Where appropriate, carbon sources were added to various minimal media at 1 g/L. SCS media was prepared by combining 100 ml of 10× YDM-base and 10 ml of 100× YDM-trace metals in 1 L of water and adjusting the pH to 5.5 with HCl and filter sterilizing. 10× YDM-base consists of (per liter) 50 g (NH₄)₂SO₄, 30 g KH₂PO₄, 5 g MgSO₄ heptahydrate, adjusted to pH 5.5 with NaOH and filter sterilized. 100× trace metals consist of (per liter) 1.5 g EDTA, 450 mg ZnSO₄ heptahydrate, 100 mg MnCl₂ tetrahydrate, 30 mg CoCl₂ hexahydrate, 30 mg CuSO₄ pentahydrate, 40 mg Na₂MoO₄ dihydrate, 450 mg CaCl₂ dihydrate, 300 mg FeSO₄ heptahydrate, and 10 mg KI, filter sterilized¹⁵. Although SCS media contains EDTA, a potential alternative source of carbon, the final concentration of this compound, 15 mg/L, is theoretically below the level required for growth. Nevertheless, all growth assays with SCS media were also performed with SCS media without added penicillin or carbenicillin as a negative control to confirm that this medium did not support growth. To completely rule out the potential contribution of EDTA to growth, experiments were also repeated in M9 media, which does not include any carbon-containing ingredients, including EDTA. M9 media was prepared by combining (per liter) 200 ml 5× M9 salts (Sigma, M6030), 2 ml 1 M MgSO₄, and 100 µl 1 M CaCl₂ in 1 L of water and adjusting the pH to 7 or 5.5 and filter sterilizing. 5× M9 salts consists of (per liter) 33.9 g Na₂HPO₄ heptahydrate, 15 g KH₂PO₄, 5 g NH₄Cl, 2.5 g NaCl in a liter of water sterilized by autoclaving. Antibiotic resistance testing was performed in LB media in the presence of 1 g/L of the indicated antibiotic. Starter cultures grown for 1 (ABC07) to 2 (ABC02, ABC08, and ABC10) d with shaking at room temperature (*ca.* 22–26 °C) were inoculated (2 µl) into LB media containing antibiotics and cultured aerobically for 2 d at room temperature before reading OD₆₀₀ reading on a PowerWave HT microplate spectrophotometer (Biotek, Inc.). All growth experiments included triplicate independent cultures, and OD₆₀₀ values were evaluated as averages with standard error unless otherwise noted.

ABC strains carbon source growth studies. For growth on diverse carbon sources, Biolog Phenotype Microarray Plates PM1 and PM2A (Hayward, CA) were used. ABC02, ABC07, ABC08, and ABC10 starter cultures were inoculated directly from frozen stocks and incubated with aeration at room temperature in 5 ml SCS media with 1 g/L carbenicillin (ABC02) or penicillin (ABC07, ABC08, and ABC10) until cultures turned visibly turbid (visible turbidity corresponds roughly to OD₆₀₀ values ~1.5 to 3 AU, approximately 3 d of growth). Each culture was washed a total of five times in SCS media lacking a carbon source by pelleting the cells (3,000 rcf, 5 min) and aspirating supernatants to remove residual glycerol or other potential carbon sources. After the final wash the cultures were resuspended in 20 ml SCS media to an OD₆₀₀ of 0.1 AU, and 100 µl per well was added to the dry Biolog plates, which were mixed by repeated pipetting. Plates were incubated at room temperature for 96 h, and growth was determined by subtraction of each well's individual initial OD₆₀₀ reading from its final reading as measured on a Powerwave HT microplate spectrophotometer (Biotek, Inc.).

Cultures for growth curves of soil isolates grown in M9 media with β-lactam antibiotics were prepared as described above with media pH adjusted to 5.5 with NaOH. A 96-well plate (COSTAR, 3595) containing 200 µl/well of M9 media with 0.25 g/L, 0.5 g/L, or 1 g/L penicillin was inoculated in triplicate with 2 µl of thrice washed cells and sealed with a Breathe-Easy membrane (Sigma-Aldrich, Z380059). Growth was monitored every 20 min at 600 nm in a PowerWave HT microplate spectrophotometer (Biotek, Inc.) at 25 °C with constant shaking (medium setting, r.p.m. not available) for 1 week. Growth data were plotted using GraphPad Prism version 7.01 for Windows (GraphPad Software, La Jolla, CA, USA).

Generation and testing of ABC07 knockout strains. Generation of the ABC07 *paaF* and penicillin *put* operon (*bla/put2/mfs/put1*) knockout strains was performed following the protocol of Hmelo et al.²⁶ using the pEXG2 plasmid⁴⁶ containing *ca.*

1,000 base pair flanking regions from around *paaF* and the *put* operon separated by a *tetA* open reading frame (see Supplementary Table 4 for primer sequences). DNA fragments were amplified by polymerase chain reaction with Q5 hotstart master mix polymerase (NEB, M04941) using ABC07 genomic DNA as template and ligated via Gibson assembly master mix (NEB, E2611S) according to the manufacturer's guidelines. Constructs were confirmed by Sanger sequencing (Genewiz) and introduced into strain ABC07 by biparental mating using *E. coli* S17 λpir followed by selection on LB agar plates containing gentamicin at 60 µg/ml. Merodiploids were selected for using VBMM agar consisting of 1.5% agar in (per liter) 200 mg MgSO₄ heptahydrate, 2 g of citric acid, 10 g of K₂HPO₄, and 3.5 g of NaNH₄HPO₄ tetrahydrate, and counter-selection was performed on LB agar containing 15% (w/v) sucrose. Loss of the gentamicin resistance cassette marker of pEXG2, loss of the target gene, and gain of *tetA* were confirmed by routine PCR using 2× ReddyMix master mix (Thermo Fisher Scientific AB0575DCLDA) according to the manufacturer's guidelines. Briefly, inserts were amplified with 25 cycles of denaturing at 94 °C for 45 s, annealing at 60 °C for 45 s, and extending at 72 °C for 2 min.

For the assay, overnight cultures of wild-type, *paaF*, and *put* ABC07 strains were grown in LB at 28 °C and washed three times in M9 media with no carbon as described above. Glucose, phenylacetic acid, and penicillin in M9 media were initially prepared at a final concentration of 0.4% (w/v), after which pH was adjusted to 5.5 with HCl for penicillin and to pH 7 for glucose and phenylacetic acid with NaOH. Media were aliquoted to 200 µl/well into a 96-well plate (COSTAR, 3595) followed by 2 µl of washed cultures and sealed with a Breathe-Easy membrane (Sigma-Aldrich, Z380059). Each strain/condition was set up in triplicate. Growth was monitored at 600 nm for 1 week with temperature maintained at 28 °C and continuous shaking on medium speed for 1 week on a PowerWave HT microplate spectrophotometer (Biotek, Inc.). OD₆₀₀ measured for each condition were plotted in GraphPad Prism version 7.01 (GraphPad Software). Further growth studies were performed as above with 1 g/L of the following carbon sources: (at pH 7) phenylacetic acid, glucose, (at pH 5.5) penicillin, benzylpenicilloic acid, 6-aminopenicillanic acid, carbenicillin, ampicillin, and cefuroxime. Optimal culture pH was determined empirically.

E. coli growth conditions. *E. coli* BL21(DE3) and *E. coli* DH10β were cultured in LB or Terrific broth (TB, MOBIO, 12105-05 or Fisher Scientific, BP9729-600) with aeration at 37 °C with 50 µg/ml kanamycin and/or 100 µg/ml carbenicillin, and 100 to 500 µM isopropyl β-D-1-thiogalactopyranoside (IPTG) when appropriate. *E. coli* W (ATCC 9637) was purchased from the American Type Culture Collection (ATCC) and propagated according to ATCC instructions or in M9 media prepared as above (adjusted to pH 7.2) with 50 µg/ml kanamycin and 100 µg/ml carbenicillin when appropriate at 28 °C. All *E. coli* strains were maintained as 15% glycerol stocks in LB at −80 °C.

Isolate whole transcriptome RNA sequencing. Genome sequencing and open reading frame calling and gene annotation. We previously published whole-genome sequences of strains ABC07, ABC08, and ABC10 (ref.²¹). Whole genome sequencing of strain ABC02 was performed exactly as for ABC07, ABC08, and ABC10. Whole-genome sequences for ABC02, ABC07, ABC08, and ABC10 (GenBank accession numbers NGUT00000000, NGUS00000000, NGUR00000000, and NGUQ00000000 respectively) were called for open reading frames and annotated as before⁴.

Preparation of cDNA and whole transcriptome RNA sequencing. Strains ABC02, ABC07, ABC08, and ABC10 were prepared for whole transcriptome RNA sequencing (RNA-seq) in triplicate for each carbon source as follows. Frozen glycerol stocks with 15% glycerol previously grown in SCS media with 1 g/L penicillin were used to inoculate 5 ml cultures of SCS media containing 1 g/L appropriate carbon source and incubated at room temperature until cultures reached turbidity visually. During this incubation period any residual glycerol is catabolized. Triplicate independent culture flasks containing 100 ml fresh SCS media with 1 g/L carbon source were then inoculated with 100 µl of turbid culture. Strains were grown with aeration at room temperature until early exponential phase at which point cells were harvested by centrifugation (3,000 rcf, 10 min). For storage before RNA extraction, cell pellets were resuspended in RNAProtect Bacteria Reagent (Qiagen, 76506) according to the manufacturer's instructions and stored at −80 °C until extraction. Total RNA was extracted via standard bead beating and phenol:chloroform protocol. Ribosomal RNA (rRNA) was depleted from the RNA extract using the Ribo-Zero rRNA Removal kit (Epicentre, MRZMB126) according to the manufacturer's instructions. Depleted RNA was converted to cDNA for sequencing via SuperScript II (Invitrogen, 18064022) as previously described⁴⁷ and sheared in a Covaris S2 (Covaris, MA, USA) to produce 150 bp fragments. Samples were sonicated in 120 µl volumes for 10 min at 10% duty cycle at intensity 5 and 100 cycles per burst.

Sheared, size-selected fragments were end-repaired and ligated with Illumina sequencing adaptors essentially as previously described⁴⁷. Single-end 1 × 50 bp sequencing was performed at the Genome Technology Access Center (GTAC, Washington University in Saint Louis) using the Illumina HiSeq 2000 platform to a target transcriptome coverage of *ca.* 10×. Raw reads have been

deposited with the Sequence Read Archive at NCBI under BioProject number PRJNA385617. Sequence reads were mapped to sequenced ABC strain genomes using Bowtie⁴⁸ with default parameters and raw expression counts were obtained using mrCounter from the RSeqTools library⁴⁹. Normalization and differential expression of open reading frames under each carbon source condition using the binomial test implementation were performed in the R package DESeq⁵⁰ following methods described by Anders and Huber for estimating variance. Genes with significantly different expression between each carbon source condition (adjusted $P < 0.00001$, DESeq) were analyzed in more detail. Highly upregulated genes from the ABC07 significant set appearing to correspond to penicillin catabolism (Fig. 2b) were plotted as normalized reads in triplicate with s.e.m. as the ratio of gene counts during growth on the given substrate to gene counts during growth on glucose using GraphPad Prism version 7.01 for Windows (GraphPad Software).

Phylogenetic analysis of upregulated amidases, hydrolases, and amidohydrolases.

Predicted amidases, hydrolases, and amidohydrolases from ABC02, ABC07, ABC08, and ABC10 that were significantly upregulated during growth on penicillin compared to glucose or histidine were targeted for phylogenetic analysis. Predicted amino acid sequences for the upregulated genes were input into the *blastp* NR database²⁸ on 8 May 2017, and the top 100 hits were combined and clustered at 70% identity using the cdhit program⁵¹. The ABC strain sequences and their top hits were combined with representative penicillin amidase sequences (E.C. 3.5.1.11) downloaded from UniProt²⁹. The combined sequences were aligned by ClustalW⁵² in the MEGA7 (ref.⁵³) program and used to construct a maximum-likelihood tree with bootstrap phylogeny test (100 rounds) and default parameters. The final tree was visualized using FigTree (<http://tree.bio.ed.ac.uk/software/figtree/>, February 2017).

The amino acid sequence of Put1 was further analyzed for the presence of a signal peptide indicative of secretion, with prediction validation using secreted β-lactamase and penicillin amidase sequences⁴³. An alignment of Put1 with *E. coli* *pga* and *pga* homologs from other bacteria was generated as above. The three-dimensional structure of Put1 was predicted based on homology using the online Phyre tool⁵⁴ with intensive settings. The resulting PDB file, as well as other PDB files, were visualized and manipulated using the PyMOL program (The PyMOL Molecular Graphics System, Version 2.0 Schrödinger, LLC.). PDB files for Put1 and *Providencia rettgeri* (1CP9)⁵⁵ and *Kluyvera citrophilia* (4PEM) penicillin amidase structures were aligned to the *E. coli* (1GK9)⁵⁶ penicillin amidase structure via the alignto command in PyMOL.

In vitro enzyme assays. put1 and put2 amplification and cloning. Inserts were amplified from ABC07 genomic DNA using the polymerase chain reaction with Iproof polymerase (Bio-Rad, 172-5330) according to the manufacturer's instructions. Briefly, inserts were amplified with 30 cycles of denaturing at 98°C for 30 s, annealing at 65°C or 60°C for 30 s, and extending at 72°C for 1.5 min using primers 5093BW and 5094BW for Put1 and 5095BW and 5096BW for Put2, respectively (Supplementary Table 4). NdeI and SacI restriction sites were introduced during PCR. Inserts and vector pET-28b(+) were digested by SacI and NdeI (New England BioLabs, R0156S and R0111S, respectively) overnight at 37°C, heat inactivated at 65°C for 20 min and purified by extraction from agarose gels followed by column clean-up (Qiagen QIAquick gel extraction kit, 28704). Inserts were ligated into vector via complementary overhang using the Fast-Link DNA Ligation kit (Epicentre, LK6201H) with a 3:1 insert to vector ratio at room temperature overnight. Ligation reactions were heat inactivated at 70°C for 10 min, dialyzed against water, and transformed by electroporation into competent *E. coli* BL21(DE3) cells using a Bio-Rad Gene Pulser XCell in 1-mm gap cuvettes at 2.0 kV, 200 Ω, and 25 μF. Cells were allowed to recover in 1 ml of rich media (SOC medium, Invitrogen 46-0821) for 1 h at 37°C and were then plated on LB agar with kanamycin. Colonies were screened for inserts by colony PCR using Thermo Scientific 2× Ready PCR Mix (Thermo Scientific, AB0575DCLDA) according to the manufacturer's instructions using vector-specific primers TSC54 and TSC55 (Supplementary Table 4). Successful colonies were cultured in LB agar with kanamycin, and plasmids were extracted by miniprep (Qiagen QIAprep Spin Miniprep kit, 27104); sequences were verified by Sanger sequencing (Genewiz).

Expression and extraction of Put1 and Put2 enzymes. For heterologous expression and purification of Put1 and Put2 from *E. coli*, 1.5 ml starter cultures of *E. coli* BL21(DE3) containing pET-28b(+) with put1 or put2 inserts were grown overnight at 37°C with aeration in TB with kanamycin. Starter cultures were used to inoculate a pair of 2.8 L Fernbach flasks containing 750 ml of TB with kanamycin for each enzyme. Cultures were incubated at 325 r.p.m. at 37°C in a MaxQ 5000 (Thermo Scientific) temperature-controlled incubator until optical densities at 600 nm (OD_{600}) of 0.2 to 0.4 AU were reached (approximately 4 h). Flasks were held on ice and IPTG was added to a final concentration of 100 (put1) or 500 (Put2) μM before flasks were returned to the shaking incubator now cooled to 25°C. The cultures were shaken overnight at 25°C for approximately 16 h to induce protein expression after which cells were harvested by centrifugation at 8,000 rcf for 15 min at 4°C in a Sorvall Legends XTR centrifuge (Thermo Scientific) in a Fiberlite F14-6×250 LE rotor (Thermo Scientific). Results of attempts to optimize Put1 expression conditions for greater yield of soluble protein can be found in

Supplementary Fig. 8. Wet cell pellets were weighed and tared on empty centrifuge tubes to find the wet cell mass. All following steps were performed at 4°C or on ice. For cell lysis, pellets were resuspended to 50% w/v in lysis buffer consisting of (per liter) 8.709 g K₂HPO₄ (50 mM), 29.22 g NaCl (500 mM), 351 μl β-mercaptoethanol (5 mM), 1.36 g imidazole (20 mM), and 100 ml glycerol (10% v/v) brought to a pH of 8 with, for Put1 purifications, addition of protease inhibitor cocktail (Thermo Scientific, A32955) according to the manufacturer's instructions. We did not observe any inhibition of amidase activity due to this addition (assayed by hydrolysis of *p*-nitroacetanilide). Suspensions were lysed using three cycles of freeze-thawing in ethanol-dry-ice baths and sonication using a Branson Sonifier 250 (Branson Ultrasonics) with microtip using the following settings: 50% duty with output adjusted to ~40% (approximately 80 W) on ice twice for 2 min until suspension viscosity was reduced. The lysed cell suspensions were clarified by centrifugation at 24,446 rcf for 30 min at 4°C in a Sorvall Legends XTR centrifuge (Thermo Scientific) in a Fiberlite F15-8×50 cy rotor (Thermo Scientific). Supernatants were decanted and stored at 4°C until purification.

Purification and storage of Put1 and Put2 enzymes. Protein purifications were carried out by immobilized metal affinity chromatography using nickel resin (Ni-NTA, Bio-Rad, 7800800) and a Bio-Rad Econo system for low-pressure chromatography with a model 2110 fraction collector (Bio-Rad, 7318122). A column was packed with 8 ml of 50% Ni-NTA resin in suspension and equilibrated in lysis buffer at 4.5 ml/min in a 4°C climate controlled room for 9 min. Clarified supernatants brought to 50 ml in lysis buffer were loaded onto the column at 4.5 ml/min 25 ml at a time with a lysis buffer wash in between each 25 ml load to decrease clogging. Lysis buffer was run through the column until UV absorbance returned to baseline levels. Proteins were eluted from the column in a gradient consisting of 0% to 100% elution buffer over 30 min. Elution buffer consists of lysis buffer with a final concentration of imidazole at 300 mM (20.42 g per liter) and NaCl at 1 M (58.44 g. per liter). Fractions were assayed for the presence of Put1 and Put2 by SDS-PAGE and, for Put1, by *p*-nitroacetanilide hydrolysis (1 mM substrate concentration) before pooling. Briefly, 7.5 μl of eluted solution was combined with 2.5 μl 4× Laemmli sample buffer (Bio-Rad, 161-0747), boiled for 10 min, loaded onto a 12% Mini-PROTEAN TGX precast gel (Bio-Rad, 456-1043), and run at 200 V for 40 min in 1× Tris/Glycine/SDS buffer (Bio-Rad, 161-0732). Gels were stained using Bio-Safe Coomassie stain (Bio-Rad, 1610796) according to the manufacturer's suggestion and visualized using a Gel-Doc XR+ (Bio-Rad). Fractions containing purified proteins were pooled and concentrated using a 10 kDa molecular weight cut-off filter (Amicon Ultra-15, UFC901024) to ca. 1 ml total volume according to the manufacturer's instructions. Elution buffer was exchanged three times using molecular weight cut-off filters as above for storage buffer consisting of (per liter) 8.709 g K₂HPO₄ (50 mM), 8.766 g NaCl (250 mM), 1 ml of 1 M dithiothreitol (1 mM) and 50 ml of glycerol (5% v/v) brought to a pH of 7.5. Final protein concentration was determined by Qubit Protein Assay kit (Thermo Scientific, Q33211), and molar enzyme concentration was found using molecular weights predicted by the EXPASY program⁵⁵. Enzymes were aliquoted in 55 μl volumes in PCR tubes on dry ice and stored at -80°C until use.

Amidase activity assays. Measurements of amidase activity using the chromogenic penicillin analog 6-nitro-3-(phenylacetamido)benzoic acid (NIPAB) and chromogenic amide *p*-nitroacetanilide were conducted as follows. NIPAB and *p*-nitroacetanilide, which have previously been validated as substrates for the detection of penicillin and other amidase activity respectively^{30,31}, were prepared in DMSO at a concentration of 200 mM and were diluted to 2 mM in phosphate buffered saline pH 7.5 (PBS, 150 mM phosphate and 50 mM NaCl). Each substrate was further diluted in a 96-well plate (COSTAR, 3595) to concentrations from 20 μM to 2,000 μM with a volume of 100 μl per well. Commercial penicillin amidase (Sigma, 76427) was diluted in PBS buffer to a concentration of 0.1 units/ml, and purified Put1 and Put2 enzymes were diluted in PBS buffer to 4 μM. To initiate reactions, 100 μl of enzyme was added to wells containing 100 μl of substrate and mixed before monitoring at 400 nm every 20 s using a PowerWave HT microplate spectrophotometer (Biotek, Inc.) with temperature maintained at 25°C. Change in absorbance over time was converted to μM min⁻¹ using the extinction coefficient for *p*-nitroacetanilide and NIPAB at pH 7.5 at 400 nm of 11,110 M⁻¹ cm⁻¹ (determined empirically) and 9,500 M⁻¹ cm⁻¹ (ref.³⁰), respectively. The Michaelis-Menten kinetics curve fit equation was solved using GraphPad Prism version 7.01 for Windows (GraphPad Software). Other chromogenic substrates were similarly assayed at 1 mM concentrations with penicillin amidase (at 0.01 U/ml) and Put1 (at 2 μM) in PBS buffer at 37°C by monitoring at 400 nm (L-glutamate 1-(*p*-nitroaniline), L-glutamate γ-(*p*-nitroaniline), and Nα-benzoyl-DL-arginine *p*-nitroaniline) or at 295 nm (N-phenylacetyl-*p*-aminobenzoate).

Indirect measurement of penicillin and benzylpenicilloic acid hydrolysis was performed by derivatization of the resulting primary amine by the reagent 4-nitro-7-chloro-benzo-2-oxa-1,3-diazole (NBD-Cl) as previously published⁴⁰. Penicillin or benzylpenicilloic acid were diluted to 2 mM in PBS buffer with 5 μM Put1 or 100 U/ml penicillin amidase and allowed to incubate overnight at 37°C. Reactions were quenched by addition of two volumes of cold acetonitrile followed by addition of 4 mM NBD-Cl in acetonitrile and incubation at 37°C for 2.5 h. Fluorescence of reactions, 250 μl in a 96-well plate (COSTAR, 3595), was read using a PowerWave

HT microplate spectrophotometer (Bioteck, Inc.) with excitation at 485 nm and emission at 538 nm with default gain.

Direct measurements of penicillin and benzylpenicilloic acid enzymatic hydrolysis were performed by a modification of a pH-dependent, colorimetric, hydrolase assay responsive to cleavage of either amide bonds³⁶. Briefly, hydrolysis of amide bonds was monitored by color change of the pH indicator *p*-nitrophenol or *m*-nitrophenol in response to protons released due to the appearance of new carboxylic acid residues following amide hydrolysis (phenylacetic acid in the case of penicillin and benzylpenicilloic acid). Reaction buffer for penicillin assays was prepared by diluting 200 mM *p*-nitrophenol in DMSO to a final concentration of 550 μM in 5 mM 3-(*N*-morpholino)propanesulfonic acid (MOPS) buffer and adjusting to a pH of 7.2 with dilute HCl and NaOH. Penicillin substrate was prepared by diluting 200 mM penicillin in DMSO to 2.4 mM in reaction buffer and adjusting the pH to 7.2 followed by dilution in triplicate in a 96-well plate (COSTAR, 3595) at concentrations ranging from 24 μM to 1.2 mM in 100 μl of *p*-nitrophenol reaction buffer. Enzymes were diluted into *p*-nitrophenol reaction buffer and brought to a pH of 7.2. *E. coli* penicillin G amidase (Sigma, 76427) and *B. cereus* β-lactamase (Sigma, P0389) were diluted to 0.1 U/ml and 0.2 U/ml, respectively, and Put1 enzyme was prepared at 4 μM. Reactions were initiated by addition of 100 μl of enzyme to 100 μl of substrates in wells. Kinetics were monitored as before with the exception that data from absorbance at 404 nm was collected. Change in absorbance over time was converted to μM/min as described elsewhere³⁶. Data were fit to Michaelis–Menten curves as before. Benzylpenicilloic acid hydrolysis was assayed as with penicillin with the following alterations. Instead of MOPS media containing *p*-nitrophenol, a buffer consisting of 10 mM *m*-nitrophenol at pH 8.4 was used with conversion of absorbance to μM/min calculated using an extinction coefficient of 1,241.5 M⁻¹ cm⁻¹ at 415 nm (determined empirically). *E. coli* penicillin G amidase (Sigma, 76427) was used at a final concentration of 5 U/ml and Put1 was used at a final concentration of 2 μM. A higher pH was required because of competition for proton signal from the alkaline amino group of penicic acid³⁷. Change in signal represents the hydrolysis of the phenylacetamide bond only as the penicillin β-lactam ring is already hydrolyzed in benzylpenicilloic acid. Because benzylpenicilloic acid lacks a β-lactam ring the activity of β-lactamase was not assayed.

Direct degradation of benzylpenicilloic acid and penicillin were followed by liquid chromatography tandem mass spectrometry (LC–MS) analysis of quenched enzymatic reactions. Reactions were conducted in 135 μl of PBS buffer at pH 7.5 with 40 μM Put1 or 0.05 U/ml *E. coli* penicillin G amidase (Sigma, 76427). To initiate reactions, 1 μl of 200 mM penicillin or benzylpenicilloic acid in DMSO was added to each reaction on ice, for a final concentration of ca 1.5 mM substrate. Aliquots of the reaction were quenched after 30 min, 5 h, and 22.5 h by removing 25 μl aliquots into 50 μl ice-cold acetonitrile to precipitate enzymes. Quenched samples were analyzed by LC–MS at the Donald Danforth Plant Sciences Institute using a Scherzo C18 column with buffers consisting of 0.1% formic acid in water (buffer A) or acetonitrile (buffer B). Analytes were eluted using a gradient method consisting of 4 min isocratic with 0% buffer B and a ramp up to 100% buffer B over 12 min. Mass spectra were recorded on a Q-Exactive mass spectrometer (Thermo Scientific) in polarity switching mode at a resolution of 140,000 (at *m/z* 200). Phenylacetic acid is not detectable using this method. Benzylpenicilloic acid spontaneously forms a pair of diastereomers that appear as two peaks under these conditions²⁵.

***E. coli* gain of function assays.** *E. coli* penicillin G amidase and ABC07 put operon cloning. For gain of function experiments, the *E. coli* W penicillin amidase (*pga*) open reading frame was cloned into the β-lactamase (*bla*) containing pZA11 expression vector⁵⁶ with its 5' secretion signal truncated by six residues at the N terminus³². Inserts were amplified by PCR using Q5 hotstart master mix polymerase (NEB, M0494L) according to the manufacturer's guidelines using primer pair 5777TSC/5779TSC (Supplementary Table 4). Linear pZA11 was prepared by inverse PCR as above using the primer pair 5780TSC/5781TSC (Supplementary Table 4). Inserts and vector were gel purified (Qiagen QIAquick gel extraction kit, 28704) and prepared for ligation by overnight double digestion with KpnI-HF and PstI-HF restriction enzymes (NEB; R3142S and R3140S, respectively), treatment with Antarctic phosphatase (vector only, NEB, M0289S), and final purification by column clean-up (Qiagen QIAquick PCR purification kit, 28104). Ligation was performed with a 2:1 insert to vector ratio using the Fast-Link DNA Ligation kit (Epicentre, LK6201H) at room temperature for 30 min followed by heat inactivation at 70 °C for 15 min. Transformation was carried out by heat shock at 42 °C of 5 μl of ligation product into 50 μl calcium competent *E. coli* W followed by recovery for 30 min at 37 °C and plating on to LB agar with 100 μg/ml carbenicillin. Colonies were screened for inserts using colony PCR with Thermo Scientific 2× Ready PCR Mix (Thermo Scientific, AB0575DCLDA) according to the manufacturer's instructions. Briefly, inserts were amplified for 30 cycles of denaturing at 94 °C for 45 s, annealing at 60 °C for 45 s, and extending at 72 °C for

2 min using vector-specific primers 22TSC and 5723TSC (Supplementary Table 4). Successful colonies were cultured in LB with carbenicillin, plasmids were extracted by miniprep (Qiagen QIAprep Spin Miniprep kit, 27104) and inserts were verified by Sanger sequencing (Genewiz). Following sequencing, a single base deletion was discovered in the first ~8 bp of the *pga* gene resulting in a frame-shift mutation. Expression from a downstream alternate in-frame start codon resulted in a product lacking the first six residues of the signal peptide. Attempts to re-clone the wild-type gene failed due to toxicity issues arising from overexpression in pZE21. Cloning of the ABC07 *put* operon into pZE21 (ref.⁵⁶) was performed similar to *pga* but via blunt-end ligation using the Fast-Link DNA Ligation kit (Epicentre, LK6201H) according to manufacturer's instructions. Stocks were maintained in LB with 15% glycerol at -80 °C.

***E. coli* W penicillloid catabolism assay.** *E. coli* W strains harboring the empty pZA11 vector or pZA11–*E. coli* *pga* and empty pZA11/pZE21 or pZA11/pZE21-*put* operon were cultured in LB supplemented with carbenicillin or carbenicillin and kanamycin overnight at 37 °C. Cells were washed three times before inoculation in M9 media as before. M9 media containing penicillin or benzylpenicilloic acid as a sole carbon source at 4 g/L was added to a 96-well plate in 200 μl aliquots followed by 2 μl of washed cells in triplicate. Plates were sealed with a Breathe-Easy membrane (Sigma-Aldrich, Z380059), and growth kinetics were monitored at 600 nm every hour using a PowerWave HT microplate spectrophotometer (BioTek, Inc.) at 28 °C with constant shaking on medium for 120 h (5 d). Growth data were plotted and evaluated for significance using GraphPad Prism version 7.01 for Windows (GraphPad Software) using pair-wise ANOVA tests with Bonferroni correction for multiple comparisons.

Reporting Summary. Further information on experimental design is available in the Nature Research Reporting Summary.

Data availability. ABC02 (this paper) and ABC07, ABC08, and ABC10 (ref.²¹) WGS short-read raw data, assembled genomes, and RNA-seq short-read data have been deposited to NCBI under BioProject number PRJNA385617 with BioSample numbers SAMN06915397, SAMN06915398, SAMN06915399, and SAMN06915400, respectively. Whole genome sequences may be found for ABC02, ABC07, ABC08, and ABC10 at DDBJ/ENA/GenBank under the accession numbers NGUT00000000, NGUS00000000, NGUR00000000, and NGUQ00000000, respectively.

References

46. Rietsch, A., Vallet-Gely, I., Dove, S. L. & Mekalanos, J. J. ExsE, a secreted regulator of type III secretion genes in *Pseudomonas aeruginosa*. *Proc. Natl Acad. Sci. USA* **102**, 8006–8011 (2005).
47. Yoneda, A., Wittmann, B. J., King, J. D., Blankenship, R. E. & Dantas, G. Transcriptomic analysis illuminates genes involved in chlorophyll synthesis after nitrogen starvation in *Acaryochloris* sp. CCME 5410. *Photosynth. Res.* **129**, 171–182 (2016).
48. Langmead, B., Trapnell, C., Pop, M. & Salzberg, S. L. Ultrafast and memory-efficient alignment of short DNA sequences to the human genome. *Genome Biol.* **10**, R25 (2009).
49. Habegger, L. et al. RSEQtools: a modular framework to analyze RNA-Seq data using compact, anonymized data summaries. *Bioinformatics* **27**, 281–283 (2011).
50. Anders, S. & Huber, W. Differential expression analysis for sequence count data. *Genome Biol.* **11**, R106 (2010).
51. Huang, Y., Niu, B., Gao, Y., Fu, L. & Li, W. CD-HIT Suite: a web server for clustering and comparing biological sequences. *Bioinformatics* **26**, 680–682 (2010).
52. Thompson, J. D., Higgins, D. G. & Gibson, T. J. CLUSTAL W: improving the sensitivity of progressive multiple sequence alignment through sequence weighting, position-specific gap penalties and weight matrix choice. *Nucleic Acids Res.* **22**, 4673–4680 (1994).
53. Kumar, S., Stecher, G. & Tamura, K. MEGA7: Molecular Evolutionary Genetics Analysis version 7.0 for bigger datasets. *Mol. Biol. Evol.* **33**, 1870–1874 (2016).
54. Kelley, L. A., Mezulis, S., Yates, C. M., Wass, M. N. & Sternberg, M. J. The Phyre2 web portal for protein modeling, prediction and analysis. *Nat. Protoc.* **10**, 845–858 (2015).
55. Gasteiger, E. et al. ExPASy: The proteomics server for in-depth protein knowledge and analysis. *Nucleic Acids Res.* **31**, 3784–3788 (2003).
56. Lutz, R. & Bujard, H. Independent and tight regulation of transcriptional units in *Escherichia coli* via the LacR/O, the TetR/O and AraC/I1-I2 regulatory elements. *Nucleic Acids Res.* **25**, 1203–1210 (1997).

Life Sciences Reporting Summary

Nature Research wishes to improve the reproducibility of the work that we publish. This form is intended for publication with all accepted life science papers and provides structure for consistency and transparency in reporting. Every life science submission will use this form; some list items might not apply to an individual manuscript, but all fields must be completed for clarity.

For further information on the points included in this form, see [Reporting Life Sciences Research](#). For further information on Nature Research policies, including our [data availability policy](#), see [Authors & Referees](#) and the [Editorial Policy Checklist](#).

► Experimental design

1. Sample size

Describe how sample size was determined.

No sample size calculations were performed. Triplicate cultures were used with bacterial growth results being uniform enough to provide necessary statistical support.

2. Data exclusions

Describe any data exclusions.

No data were excluded

3. Replication

Describe whether the experimental findings were reliably reproduced.

All experiments were replicated at least once.

4. Randomization

Describe how samples/organisms/participants were allocated into experimental groups.

Randomization was not necessary in our study as it is not applicable to bacterial cultures.

5. Blinding

Describe whether the investigators were blinded to group allocation during data collection and/or analysis.

Blinding was not necessary for our study and was not performed.

Note: all studies involving animals and/or human research participants must disclose whether blinding and randomization were used.

6. Statistical parameters

For all figures and tables that use statistical methods, confirm that the following items are present in relevant figure legends (or in the Methods section if additional space is needed).

n/a Confirmed

- The exact sample size (*n*) for each experimental group/condition, given as a discrete number and unit of measurement (animals, litters, cultures, etc.)
- A description of how samples were collected, noting whether measurements were taken from distinct samples or whether the same sample was measured repeatedly
- A statement indicating how many times each experiment was replicated
- The statistical test(s) used and whether they are one- or two-sided (note: only common tests should be described solely by name; more complex techniques should be described in the Methods section)
- A description of any assumptions or corrections, such as an adjustment for multiple comparisons
- The test results (e.g. *P* values) given as exact values whenever possible and with confidence intervals noted
- A clear description of statistics including central tendency (e.g. median, mean) and variation (e.g. standard deviation, interquartile range)
- Clearly defined error bars

See the web collection on [statistics for biologists](#) for further resources and guidance.

► Software

Policy information about [availability of computer code](#)

7. Software

Describe the software used to analyze the data in this study.

Growth and enzyme kinetics data were plotted and evaluated for significance using GraphPad Prism version 7.01 for Windows (GraphPad Software, La Jolla California, USA).

For manuscripts utilizing custom algorithms or software that are central to the paper but not yet described in the published literature, software must be made available to editors and reviewers upon request. We strongly encourage code deposition in a community repository (e.g. GitHub). *Nature Methods* guidance for [providing algorithms and software for publication](#) provides further information on this topic.

► Materials and reagents

Policy information about [availability of materials](#)

8. Materials availability

Indicate whether there are restrictions on availability of unique materials or if these materials are only available for distribution by a for-profit company.

Unique materials are readily available from commercial suppliers (i.e. beznypenicilloic acid from the Sigma Aldrich collection of rare and unique chemicals).

9. Antibodies

Describe the antibodies used and how they were validated for use in the system under study (i.e. assay and species).

No antibodies were used in this study.

10. Eukaryotic cell lines

a. State the source of each eukaryotic cell line used.

No eukaryotic cells were used in this study

b. Describe the method of cell line authentication used.

No eukaryotic cells were used in this study

c. Report whether the cell lines were tested for mycoplasma contamination.

No eukaryotic cells were used in this study

d. If any of the cell lines used are listed in the database of commonly misidentified cell lines maintained by [ICLAC](#), provide a scientific rationale for their use.

No eukaryotic cells were used in this study

► Animals and human research participants

Policy information about [studies involving animals](#); when reporting animal research, follow the [ARRIVE guidelines](#)

11. Description of research animals

Provide details on animals and/or animal-derived materials used in the study.

No animals were used in this study

Policy information about [studies involving human research participants](#)

12. Description of human research participants

Describe the covariate-relevant population characteristics of the human research participants.

No human subjects were used in this study